Analysis and Synthesis of Underactuated Compliant Mechanisms Based on Transmission Properties of Motion and Force

Wenrui Chen, Caihua Xiong, and Yaonan Wang

***Abstract*—This article analyzes and designs the transmission structure for underactuated compliant mechanisms (UCMs). The transmission structure of UCMs consists of serial and parallel transmission chains. At first, the UCMs are classified systematically according to the number and distribution of the serial and parallel transmissions. Next, the active and passive transmission properties of motion and force in UCMs are analyzed on the defined four subspaces of tangent and cotangent spaces of joint space. Synthesizing the classification and the transmission properties of UCMs, the congruent relationship between mechanical structure and transmission function is established, and different cases of UCMs are discussed and compared. A novel type of UCMs can achieve the independent regulation of passive stiffness, active force, and active motion that is useful for improving the transmission performance in robotic and prosthetic hands. Finally, a functional oriented design method is proposed and used to design a single-actuator two-fingered gripper for enveloping and precision grasps. The results demonstrate the validity of the proposed method.**

***Index Terms*—Classification, design, mechanical compliance, transmission structure, underactuated mechanisms.**

I. Introduction

GIVING robots the ability to perform functional movements and to exert forces effectively on the external environment is a fundamental task in robot design. The most straightforward strategy is to use the fully actuated method with each robot joint driven independently by the actuators. In principle, fully independent actuation offers the widest possibilities, limited only by the robot kinematics. However, this design is difficult to effectively integrate and control in many situations such as multifingered dexterous hands and micromobile robots. The other alternative is *underactuated mechanism*, with fewer actuators than the degrees of freedom (DOFs), offloading some of control to the physical structure. The design of the underactuated mechanism is to embed mechanical intelligence [1] into the transmission, thereby giving the mechanical system the ability to passively adapt to the external environment in both motion and force. Usually, to keep the mechanisms from incoherent motion, it is embedded with passive elements, such as mechanical limits, clutches, and springs. Among them, *mechanical compliance* is of particular concern, because it can conform passively to the external environment and improve the stability and robustness of transmission. Because of its mechanical adaptability [2], bioimitability [3], and simple control, *underactuated compliant mechanisms* (UCMs) have been widely used in design of robots such as walking robots [4]–[6], flapping-wing aerial robots [7]–[9], and rehabilitation robots [10]–[12]. Especially in robotic and prosthetic hands [13]–[16], the underactuated hands do not only achieve enveloping grasp, but also are expected to perform dexterous functions like human hands, such as precision grasp [17] and in-hand manipulation [18]. In underactuated robots, the underactuation and compliance transform the control complexity based on sensing driven into the design complexity based on mechanical adaptation.

In compliant underactuated manipulation systems, there exist uncontrollable movements and forces [19], which may lead to undesirable results such as ejection phenomenon [20], namely that a grasp sequence can degenerate into ejecting the object. To improve the performance of force and motion, an effective method is to optimize the transmission. The design of transmission includes structure design and parameter design. Existing optimization methods generally only optimize the parameters of a given transmission structure. Birglen and Gosselin [21] focused on optimizing geometric parameters of linkages that generate positive contact forces in the maximum configuration space. Dollar and Howe [22] optimized the joint compliant coupling of an underactuated gripper in order to maximize successful grasp range and minimize contact forces for a wide range of target object sizes and positions. However, a good

Manuscript received June 20, 2019; accepted December 28, 2019. Date of publication March 3, 2020; date of current version June 4, 2020. This work was supported in part by the National Natural Science Foundation of China under Grant 61733004, Grant 51335004 and Grant 91648203, in part by Hunan Key Laboratory of Intelligent Robot Technology in Electronic Manufacturing under Grant IRT2018005, and in part by the Fundamental Research Funds for the Central Universities under Grant 531107051013. *(Corresponding authors: Wenrui Chen; Caihua Xiong.)*

W. Chen and Y. Wang are with the School of Robotics, Hunan University, Changsha 410082, China, and also with the National Engineering Laboratory for Robot Vision Perception and Control, Changsha 410082, China (e-mail: chenwenrui@hnu.edu.cn; yaonan@hnu.edu.cn).

C. Xiong is with the State Key Laboratory of Digital Manufacturing Equipment and Technology, Institute of Rehabilitation and Medical Robotics, Huazhong University of Science and Technology, Wuhan 430074, China (e-mail: chxiong@hust.edu.cn).

This article has supplementary downloadable material available at http://ieeexplore.ieee.org, provided by the authors. The material consists of a video, viewable with Windows Media Player. The attached video shows: 1) the designed prototype gripper with one actuator and two fingers; 2) measure experiments of enveloping grasping and parallel grasping; and 3) examples of grasping executed by the prototype gripper. The size of the video is 27.5 MB.

Color versions of one or more of the figures in this article are available online at http://ieeexplore.ieee.org.

Digital Object Identifier 10.1109/TRO.2019.2963650

structure design could achieve effects that cannot be achieved by parameter optimization alone.

The development of transmission structures of UCMs follows mainly two themes, namely, design for simplifying control [23]–[25] and bionics [26]. A prototype robotic hand explicitly utilizing underactuation was presented for the first time by Hirose and Umetani [27] for softly and gently conforming to objects of any shape and holding them simply actuated by a pair of tendons. Hirose's gripper adopted a differential mechanism (DM). After that, different implementation forms of underactuated mechanisms were used in robots such as linkage [13], gear [28], continuum mechanism [29], and soft structure [16]. Taking inspiration from the *synergy* of human hand [30]–[32], much work has been done in designing anthropomorphic hands with few inputs [33]–[35]. For example, Brown and Asada [33] designed a mechanical hand to restructure the first two posture synergies with two actuators driving 17 joints of the whole hand via a coupling mechanism (CM). To solve force indeterminacies in the kinematic model of synergies, soft synergy was introduced [36]. The soft synergy is actually a CM embedded with mechanical compliance. Catalano *et al.* [35] found that there is an equivalent relationship between DM and CM, and then built the Pisa/IIT SoftHand implementing the soft synergy via a differential mechanism with flexible joints (DM-FJ). In fact, among different types of UCMs, there are not only close correlations but also significant differences with respect to the transmission characteristics of force and motion.

In the transmission structure of UCMs, mechanical compliance can be arranged in two distinct ways: in series with the actuators (e.g., series elastic actuators) and parallel to the actuators (e.g., flexible joints). The series compliance, introduced through series elastic actuators, has been studied extensively [37] and applied in many robotic systems for reduced actuator impedance [38], better collision safety [39], and improved force control [37]. Variable stiffness actuators have built upon this idea to simultaneously control the output joint torques and mechanical stiffness [40]. The parallel compliance improves stability and robustness to impact during grasping [41] and dexterous manipulation tasks [42]. Parallel compliance was also used in underactuated fingers of the SDM hand [14] to enable successful grasping with uncertainty in target object location. Usually, both series and parallel springs exist in a UCM. However, there are few studies on the comprehensive analysis and discussion of series and parallel compliance in mechanical system, involving the transmission characteristics of force and motion.

This article presents a methodology to analyze and design the transmission structures of UCMs. The closest work to this article is in [21] and [43]. Birglen and Gosselin [21] focused on serial transmissions in DMs and provided a tool to analyze and compare different forms such as linkages, tendon pulleys, and gears. The analysis and design in [43] were developed for tendon-driven mechanisms, and could not distinguish between serial and parallel structures and active and passive functions. In our work, the analysis and design methodology of UCMs is proposed on the relationship between the mechanical structure of serial and parallel compliance and the active and passive transmission properties of force and motion. The main contributions of our work are as follows.

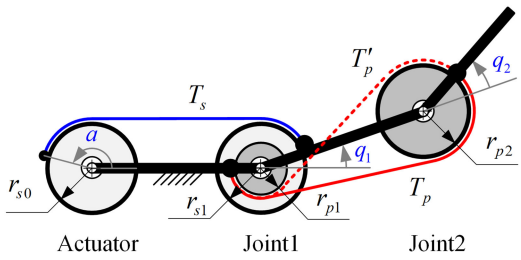

Fig. 1. Serial transmission (a blue line) and two variants of a parallel transmission (two red lines) in an underactuated mechanism.

1) A systematic classification of UCMs is proposed. This classification is based on the number and distribution of serial and parallel transmission chains.
2) Active and passive transmission properties of UCMs are revealed through the annihilator and dual relationship in the tangent space and the cotangent space of joint space. The transmission properties describe completely the characteristics of force and motion in UCMs.

In this article, the classification and the transmission properties of UCMs are synthesized, the congruent relationship between mechanical structure and transmission function is established, and different cases of UCMs are analyzed and compared. Based on the analysis of transmission structure of UCMs, a functional oriented design method is proposed and implemented in a two-fingered gripper for enveloping and precision grasps.

This article is organized as follows. Section II introduces the unified kinematic model of UCMs and analyzes its stability. Section III classifies underactuated mechanisms based on the structure and distribution of the serial and parallel transmissions. We analyze the transmission properties of motion and force of UCMs in Section IV and establish the relationship between the mechanical structures and the transmission functions of the UCMs in Section V. Section VI gives a design method of UCMs based on the transmission principles and verifies the effectiveness of the proposed method via an example. Finally, Section VII concludes this article.

II. Unified Kinematic Description of Transmissions

A. Kinematics of Transmission

Consider an underactuated mechanism with n-DOFs driven by m actuators. Let $\mathbf{a} \in \Re^m$ and $\mathbf{q} \in Q \subseteq \Re^n$ be actuator coordinates and joint angle vectors, respectively. The joints and actuators are constrained by l transmissions. The transmission variable $\mathbf{T} \in \Re^l$ is expressed as

$$\mathbf{T} = \mathbf{T}(\mathbf{q}, \mathbf{a}) = \begin{bmatrix} \mathbf{T}_s(\mathbf{q}, \mathbf{a}) \\ \mathbf{T}_p(\mathbf{q}) \end{bmatrix} \tag{1}$$

where $\mathbf{T}_s \in \Re^{l_s}$ is the transmission variable in series with the actuators, and $\mathbf{T}_p \in \Re^{l_p}$ is the transmission variable in parallel to the actuators, as shown in Fig. 1. l_s and l_p are the numbers of serial and parallel transmissions, respectively. The sum of l_s and l_p is l

$$l_s + l_p = l. \tag{2}$$

Note that the transmission variables $\mathbf{T}$ are the deformation amounts of the transmissions. Thus, the transmission variables in series with the actuators are expressed as functions with respect to $\mathbf{a}$ and $\mathbf{q}$, whereas the parallel transmission variables are only related with $\mathbf{q}$, as shown in (1). In this article, the positive deformation indicates elongation, whereas the negative value represents compression. If a transmission is embedded using a spring, the transmission variable is the elongation of the spring. If a transmission is rigid such as a rigid gear chain, the transmission variable is constant, specified as zero here.

Example 1: An underactuated mechanism with an actuator and two joints is shown in Fig. 1. The serial transmission variable T_s is the elongation of the rope, expressed as

$$T_s = r_{s0}a - r_{s1}q_1$$

where r_{s0} and r_{s1} are the corresponding pulley radii, respectively. If the rope deformation is not taken into account, $T_s = 0$. The parallel transmission variable T_p is

$$T_p = r_{p1}q_1 + r_{p2}q_2$$

where r_{p1} and r_{p2} are the corresponding pulley radii, respectively. When the routing direction of the rope on the pulley changes, the transmission equation also changes. The transmission variable T_p' in Fig. 1 is

$$T_p' = r_{p1}q_1 + (-r_{p2})q_2.$$

Comparing the transmission equations of T_p and T_p', it is not hard to find that the routing direction of the rope on the pulley r_{p2} affects the sign in front of the corresponding pulley radius in the transmission equation. Thus, these two routing methods can be represented by either of the above two equations when the domain of r_{p2} is defined as $r_{p2} \in \Re$. The absolute value of r_{p2} is the pulley radius, and the sign represents the routing direction of the rope on the pulley. $r_{p2} = 0$ means there is no pulley or the rope passes through the axle. If not specified in this article, the displayed routings in the examples are selected in such a way that the parameters of the pulley radius r_i are positive in the corresponding equations.

The derivative of the transmission variables is expressed as

$$\begin{bmatrix} \delta\mathbf{T}_s \\ \delta\mathbf{T}_p \end{bmatrix} = \begin{bmatrix} \mathbf{J}_{s1} & \mathbf{J}_{s2} \\ \mathbf{J}_p & \mathbf{0} \end{bmatrix} \begin{bmatrix} \delta\mathbf{q} \\ \delta\mathbf{a} \end{bmatrix} \tag{3}$$

where the transmission Jacobian matrices $\mathbf{J}_{s1} = \frac{\partial \mathbf{T}_s}{\partial \mathbf{q}} \in \Re^{l_s \times n}$, $\mathbf{J}_{s2} = \frac{\partial \mathbf{T}_s}{\partial \mathbf{a}} \in \Re^{l_s \times m}$, and $\mathbf{J}_p = \frac{\partial \mathbf{T}_p}{\partial \mathbf{q}} \in \Re^{l_p \times n}$. Then, from the virtual work principle, the *equilibrium equation* of this transmission mechanism is given as

$$\begin{bmatrix} \tau \\ \mathbf{f}_a \end{bmatrix} = \begin{bmatrix} \mathbf{J}_{s1}^T & \mathbf{J}_p^T \\ \mathbf{J}_{s2}^T & \mathbf{0} \end{bmatrix} \begin{bmatrix} \mathbf{f}_{\mathbf{T}s} \\ \mathbf{f}_{\mathbf{T}p} \end{bmatrix} \tag{4}$$

where $\mathbf{f}_{\mathbf{T}s}$ is a force generated in the serial transmission, $\mathbf{f}_{\mathbf{T}p}$ is a force generated in the parallel transmission, $\mathbf{f}_a$ is the actuator force, and τ is the external force described in joint space. The external force may be from the contact with the environment in robotic hands and walking robots, or from the aerodynamic drag in flapping wing robots.

B. Stability of UCMs

Next, consider serial and parallel transmissions that utilize elastic mechanisms in their construction. Elastic elements in the serial transmissions are called serial springs, and elastic elements in the parallel transmissions are called parallel springs. The elastic potential energy of a UCM can be expressed as

$$V(\mathbf{q}, \mathbf{a}) = \frac{1}{2}\mathbf{T}(\mathbf{q}, \mathbf{a})^T \mathbf{K}_T \mathbf{T}(\mathbf{q}, \mathbf{a}) \tag{5}$$

where $\mathbf{K}_T = \mathrm{diag}(\mathbf{K}_s, \mathbf{K}_p) = \mathrm{diag}(k_{s1}, \ldots, k_{sl_s}, k_{p1}, \ldots, k_{pl_p})$ is a stiffness matrix, $k_{si}, i = 1, \ldots, l_s$, is the stiffness of the serial springs, and $k_{pi}, i = 1, \ldots, l_p$, is the stiffness of the parallel springs. The elastic force $\mathbf{f}_T = [\mathbf{f}_{Ts}^T \ \mathbf{f}_{Tp}^T]^T$ can be expressed via the partial derivative of $V(\mathbf{T})$

$$\mathbf{f}_T = -\frac{\partial V(\mathbf{T})}{\partial \mathbf{T}} = -\mathbf{K}_T \mathbf{T}(\mathbf{q}, \mathbf{a}). \tag{6}$$

The second-order partial derivative of the elastic potential energy with respect to $(\mathbf{q}, \mathbf{a})$ is

$$\begin{bmatrix} \delta\boldsymbol{\tau} \\ \delta\mathbf{f}_a \end{bmatrix} = -\frac{\partial^2 V}{\partial(\mathbf{q}, \mathbf{a})^2} \begin{bmatrix} \delta\mathbf{q} \\ \delta\mathbf{a} \end{bmatrix} \tag{7}$$

where $\frac{\partial^2 V}{\partial(\mathbf{q},a)^2} = \left[\begin{smallmatrix} \mathbf{K}_q & \mathbf{K}_{qa}^T \\ \mathbf{K}_{qa} & \mathbf{K}_a \end{smallmatrix}\right]$ is a system stiffness matrix. Then, (7) could be rewritten as

$$\delta\boldsymbol{\tau} = -\mathbf{K}_q \delta\mathbf{q} - \mathbf{K}_{qa}\delta\mathbf{a} \tag{8}$$

$$\delta\mathbf{f}_a = -\mathbf{K}_{qa}^T \delta\mathbf{q} - \mathbf{K}_a \delta\mathbf{a}. \tag{9}$$

The complexity of the expression of the system stiffness matrix is influenced by the transmission Jacobian matrices. In order to avoid unnecessary trouble caused by the complex expression of the system stiffness matrix, consider linear transmission mechanisms such as gears and tendon pulley in this article. Then, the transmission Jacobian matrices are determined by structure parameters, nothing to do with joint angles and actuator coordinates. Thus, the system stiffness matrix is expressed as

$$\begin{cases} \mathbf{K}_q = \mathbf{J}_{s1}^T \mathbf{K}_s \mathbf{J}_{s1} + \mathbf{J}_p^T \mathbf{K}_p \mathbf{J}_p \\ \mathbf{K}_a = \mathbf{J}_{s2}^T \mathbf{K}_s \mathbf{J}_{s2} \\ \mathbf{K}_{qa} = \mathbf{J}_{s1}^T \mathbf{K}_s \mathbf{J}_{s2} \end{cases} \tag{10}$$

and the relationship of forces and coordinates of the transmission mechanism can be expressed compactly as

$$\begin{bmatrix} \tau \\ \mathbf{f}_a \end{bmatrix} = -\begin{bmatrix} \mathbf{K}_q & \mathbf{K}_{qa} \\ \mathbf{K}_{qa}^T & \mathbf{K}_a \end{bmatrix} \begin{bmatrix} \Delta\mathbf{q} \\ \Delta\mathbf{a} \end{bmatrix} \tag{11}$$

where $\Delta\mathbf{q} = \mathbf{q} - \mathbf{q}_0$, $\Delta\mathbf{a} = \mathbf{a} - \mathbf{a}_0$, $\mathbf{q}_0$ is the vector of initial joint angles, and $\mathbf{a}_0$ is the vector of the corresponding initial actuator coordinates. Therefore, $\{\mathbf{q}, \mathbf{a}\}$ is the state variable of the transmission mechanism. At the initial state $\{\mathbf{q}_0, \mathbf{a}_0\}$, there are zero external force and zero actuator force. If no otherwise specified, the initial state is set to be zero, $\mathbf{q}_0 = \mathbf{0}\ \mathbf{a}_0 = \mathbf{0}$.Then, we define an equilibrium point as follows.

Definition 1: The state $\mathbf{x} = \{\mathbf{q}, \mathbf{a}\}$ is called an equilibrium point of the transmission mechanism if the external force τ is zero at $\mathbf{x}$.

A stable equilibrium point is defined as follows.

Definition 2: If the external force generated by any infinitesimal joint displacement returns the state to the equilibrium point, then the equilibrium point is stable.

Definition 3: Transmission mechanisms are called stable transmission mechanisms if a stable equilibrium point exists. Otherwise, the transmission mechanisms are unstable.

The following theorem gives a sufficient and necessary condition to judge the stability of a transmission mechanism.

Theorem 1: The transmission mechanism is stable, if and only if $\mathrm{rank}([\,\mathbf{J}_{s1}^T\ \mathbf{J}_p^T\,]) = n$.

Proof: Because the stiffness matrix $\mathbf{K}_T$ is positive definite, the following equation always holds with respect to any vector $\mathbf{y} \in \Re^l$ and $\mathbf{y} \neq \mathbf{0}$:

$$\mathbf{y}^T \mathbf{K}_T \mathbf{y} > 0. \tag{12}$$

Denote $\mathbf{A} = [\,\mathbf{J}_{s1}^T\ \mathbf{J}_p^T\,] \in \Re^{n\times l}$. If $\mathrm{rank}(\mathbf{A}) = n$, the matrix $\mathbf{A}$ is row full rank. Thus, the transformation $\mathbf{y}_z = \mathbf{A}^T\mathbf{z}$ is injective, namely that any $\mathbf{z} \neq \mathbf{0}$ maps to a vector $\mathbf{y}_z = \mathbf{A}^T\mathbf{z} \neq \mathbf{0}$, then according to (12), we obtain

$$\mathbf{z}^T \mathbf{A}\mathbf{K}_T\mathbf{A}^T\mathbf{z} > 0.$$

So, $\mathbf{A}\mathbf{K}_T\mathbf{A}^T$, which is the matrix $\mathbf{K}_q$, is positive definite, and the transmission mechanism is stable.

If $\mathrm{rank}(\mathbf{A}) \neq n$, namely $\mathrm{rank}(\mathbf{A}) < n$, the matrix $\mathbf{A}$ is not row full rank. Thus, $\mathbf{z}_1 \neq \mathbf{0}$ let $\mathbf{y}_z = \mathbf{A}^T\mathbf{z}_1 = \mathbf{0}$, then

$$\mathbf{z}_1^T \mathbf{A}\mathbf{K}_T\mathbf{A}^T\mathbf{z}_1 = 0$$

which means that when a joint displacement along the vector $\mathbf{z}_1$ happens, the potential energy of the mechanism system does not increase to generate restoring force. Hence, the transmission mechanism is unstable. ■

According to Theorem 1, if $l_s + l_p < n$ in a UCM, it is unstable during free motion. According to (10), the stiffness matrix of joint space is

$$\mathbf{K}_q = \mathbf{A}\mathbf{K}_T\mathbf{A}^T = \begin{bmatrix} \mathbf{J}_{s1} \\ \mathbf{J}_p \end{bmatrix}^T \begin{bmatrix} \mathbf{K}_s & \\ & \mathbf{K}_p \end{bmatrix} \begin{bmatrix} \mathbf{J}_{s1} \\ \mathbf{J}_p \end{bmatrix}.$$

In a stable transmission mechanism, the matrix $[\,\mathbf{J}_{s1}^T\ \mathbf{J}_p^T\,]$ is row full rank and $\mathbf{K}_q$ is positive definite. In this article, we are mainly interested in stable transmission mechanisms.

Example 2: Consider an underactuated mechanism with two joints driven by an actuator, as shown in Fig. 3(e). There are a serial transmission and two parallel transmissions in this mechanism. Its transmission equation is

$$\begin{cases} T_{s1} = a - r_{s1}q_1 - r_{s2}q_2 \\ T_{p1} = q_1 \\ T_{p2} = q_2 \end{cases}$$

where T_{s1}, T_{p1}, and T_{p2} are the deformation amounts of the corresponding springs. According to (3), the transmission Jacobian matrices are $\mathbf{J}_{s1} = [\,-r_{s1}\ -r_{s2}\,]$, $\mathbf{J}_{s2} = 1$, and $\mathbf{J}_p = \mathbf{I}^{2\times 2}$. $\mathrm{rank}([\,\mathbf{J}_{s1}^T\ \mathbf{J}_p^T\,]) = 2$, so this transmission mechanism is stable.

According to (10), the stiffness matrix $\mathbf{K}_q$is

$$\mathbf{K}_q = \begin{bmatrix} k_{p1} + k_s r_{s1}^2 & k_s r_{s1} r_{s2} \\ k_s r_{s1} r_{s2} & k_{p2} + k_s r_{s2}^2 \end{bmatrix}$$

which is positive definite. It means that the system can return to equilibrium after the external disturbance is removed.

III. Classification of Underactuated Mechanisms

This section classifies underactuated mechanisms based on the structure and distribution of the serial and parallel transmissions.

A. Constraint of the Transmissions

Consider serial and parallel transmissions that utilize elastic mechanisms in their construction, then $l_s \geq m$. Consider the serial transmissions independent of each other. If the number of serial or parallel transmissions is more than *n*, the extra transmissions can be linearly represented by the *n* transmissions. Thus, the number of serial transmissions is constrained by

$$m \leq l_s \leq n. \tag{13}$$

Likewise, the number of parallel transmissions is constrained by

$$0 \leq l_p \leq n. \tag{14}$$

From Theorem 1, it is not hard to find that the stability of an underactuated mechanism is determined by the rank of the matrix $[\,\mathbf{J}_{s1}^T\ \mathbf{J}_p^T\,]$. According to the basic relationship of matrix rank, the following inequality is true:

$$\mathrm{rank}(\mathbf{J}_{s1}) + \mathrm{rank}(\mathbf{J}_p) \geq \mathrm{rank}\left(\left[\,\mathbf{J}_{s1}^T\ \mathbf{J}_p^T\,\right]\right). \tag{15}$$

According to Theorem 1, a sufficient and necessary condition for a stable mechanism is $\mathrm{rank}([\,\mathbf{J}_{s1}^T\ \mathbf{J}_p^T\,]) = n$. Thus, (15) is rewritten as

$$l_s + l_p \geq n \tag{16}$$

which means that the minimum number of transmissions is *n* for a stable underactuated mechanism.

According to (13), (14), and (16), the scope of the numbers of serial and parallel transmissions for a stable underactuated mechanism is given with a convex polygon *ABCD* in Fig. 2. According to (13) and (14), the edge *CD* is constrained by the number of serial transmissions, whereas the light gray edges *A–B–C* are constrained by the independence of serial or parallel transmissions. The black edge *AD* is constrained by the stability of the UCMs according to (16). There are two cases in (16), which are given as follows:

1) $l_s + l_p = n$: a UCM *with minimum transmissions* for stability;
2) $l_s + l_p > n$: a UCM *with redundant transmissions.*

During free motion before contacting with environment, $\tau = \mathbf{0}$. Substituting $\tau = \mathbf{0}$ into (11), the actuation force can be derived

$$\mathbf{f}_a = \left(\mathbf{K}_{qa}^T\mathbf{K}_q^{-1}\mathbf{K}_{qa} - \mathbf{K}_a\right)\Delta\mathbf{a}. \tag{17}$$

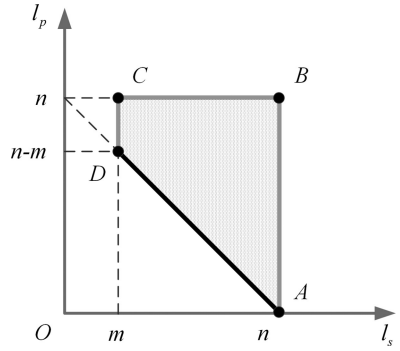

Fig. 2. Feasible interval of the numbers of serial and parallel transmissions for a stable UCM.

If $l_s + l_p = n$, then $[\mathbf{J}_{s1}^T \ \mathbf{J}_p^T] \in \Re^{n\times n}$ is a nonsingular matrix. Thus, the following equation is true:

$$\mathbf{J}_{s1} = \begin{bmatrix}\mathbf{I} & \mathbf{0}\end{bmatrix}\begin{bmatrix}\mathbf{J}_{s1}\\ \mathbf{J}_p\end{bmatrix} \tag{18}$$

then

$$\mathbf{J}_{s1}\begin{bmatrix}\mathbf{J}_{s1}\\ \mathbf{J}_p\end{bmatrix}^{-1} = \begin{bmatrix}\mathbf{I} & \mathbf{0}\end{bmatrix}. \tag{19}$$

Substituting (10) and (19) into (17), then $\mathbf{f}_a = \mathbf{0}$. Hence, a UCM with minimum transmissions $(l_s + l_p = n)$does not need the actuators to counteract the elastic force in free motion, whereas the actuation force exists in a UCM with redundant transmission $(l_s + l_p > n)$during free motion.

B. Distribution of Serial Transmissions

To analyze the serial transmissions, the elastic elements are eliminated in the underactuated mechanisms, namely the parallel springs are disconnected and the serial springs are toughened. Thus, there are not parallel transmissions but serial transmissions. Meanwhile, the serial transmissions are rigid, so $\mathbf{T}_s = \mathbf{0}$. The transmission function is expressed as

$$\mathbf{T} = \mathbf{T}_s(\mathbf{q}, \mathbf{a}) = \mathbf{0}.$$

Then, (3) is rewritten as

$$\mathbf{J}_{s1}\delta\mathbf{q} + \mathbf{J}_{s2}\delta\mathbf{a} = \mathbf{0}. \tag{20}$$

Equation (20) can be simplified under two extreme values of $l_s$in (13) as follows.

1) $l_s = n$: The matrix $\mathbf{J}_{s1} \in \Re^{n\times n}$ is reversible. Equation (20) is rewritten as

$$\delta\mathbf{q} = \mathbf{C}\delta\mathbf{a} \tag{21}$$

where the transmission matrix $\mathbf{C} = -\mathbf{J}_{s1}^{-1}\mathbf{J}_{s2}$. The joint motion is constrained in the image space of $\mathbf{C}$, and there is a one-to-one mapping between actuator coordinates and joint angles. Hence, this transmission is rigidly coupled, called CM. Fig. 3(a) conceptually illustrates a tendon-pulley CM with a motor actuating two joints, whose transmission equation is

$$\begin{cases} 0 = a - r_{s1}q_1 \\ 0 = a - r_{s2}q_2 \end{cases}.$$

TABLE I
NUMBERS OF SERIAL AND PARALLEL TRANSMISSIONS FOR FOUR BASIC CASES OF UCMS

	Differential ($l_s = m$)	Coupling ($l_s = n$)
Redundant ($l > n$)	$l_s = m,\ l_p = n$ (Case C)	$l_s = n,\ l_p = n$ (Case B)
Minimum ($l = n$)	$l_s = m,\ l_p = n - m$ (Case D)	$l_s = n,\ l_p = 0$ (Case A)

Thus, the transmission matrix is

$$\mathbf{C} = \begin{bmatrix}1/r_{s1} & 1/r_{s2}\end{bmatrix}^T. \tag{22}$$

The equilibrium equation is written as

$$\mathbf{f}_a = -\mathbf{C}^T\tau \tag{23}$$

whose inverse mapping, from actuation force to joint torque, is nonunique. It means the system is statically indeterminate. In the CM, determined motion and statically indeterminate force coexist. To deal with the statically indeterminate, compliance is generally included in the CM [44], as shown in Fig. 3(b).

2) $l_s = m$: The matrix $\mathbf{J}_{s2} \in \Re^{m\times m}$is reversible. Equation (20) is simplified as

$$\delta\mathbf{a} = \mathbf{D}\delta\mathbf{q} \tag{24}$$

where $\mathbf{D} = -\mathbf{J}_{s2}^{-1}\mathbf{J}_{s1}$. The equilibrium equation is written as

$$\tau = -\mathbf{D}^T\mathbf{f}_a. \tag{25}$$

The transmission mechanism operates on torque instead of joint motion, called DM. A tendon-pulley DM is illustrated conceptually in Fig. 3(d), whose transmission matrix is

$$\mathbf{D} = \begin{bmatrix}r_{s1} & r_{s2}\end{bmatrix}. \tag{26}$$

Equation (24) highlights the nonuniqueness of the position attained by a DM. All possible joint motions satisfying (24) for $\delta\mathbf{a} = \mathbf{0}$ span the kernel of $\mathbf{D}$. It is exactly these kernel motions that provide DMs with the adaptivity to physical environment in grasping or moving. In practice, the random kernel motion is constrained by passive elements such as springs, mechanical limits, or through the interaction with external environment such as the automobile differential maintaining traction on the bumpy ground without closed-loop control. For example, a mechanism in Fig. 3(d) is embedded with joint springs.

C. Classification of UCMs

From the above, the UCMs are classified from the following two aspects: the number of serial transmissions and the sum of serial and parallel transmissions. According to the last section, from the number of serial elastic elements, two extreme values in (13) reflect two classes of the underactuated transmission formations, namely DM $(l_s = m)$ and CM $(l_s = n)$. According to (16), the UCMs are divided into two classes: *with minimum transmissions* $(l = n)$ for stability, and *with redundant transmissions* $(l > n)$. We can get four cases of UCMs by combining the two taxonomies, as shown in Table I. Four vertices, *A*, *B*, *C*, and *D*, of the feasible region in Fig. 2 represent the four cases shown in Table I. The feasible region *ABCD* is a convex quadrangle so

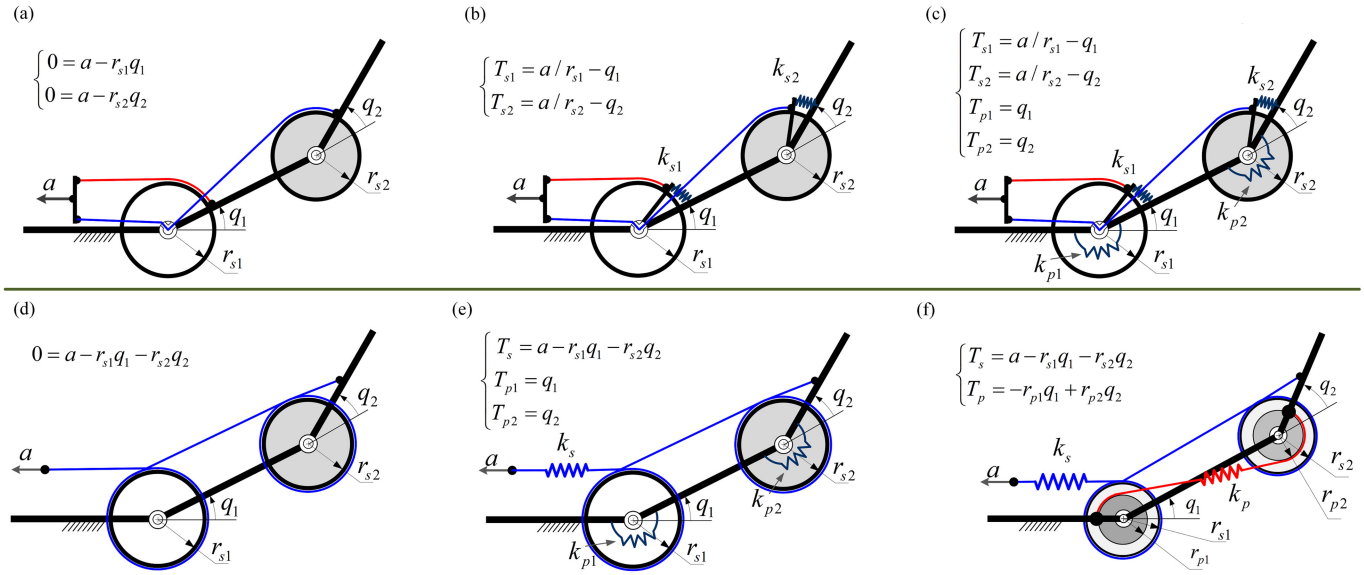

Fig. 3. Six cases of underactuated mechanisms illustrated with one-actuator two-jointed mechanisms. Note that the transmission equations are given in the corresponding figures, and the transmission variables T_s and T_p are the elastic deformation amounts of the corresponding springs. (a) CM. (b) SCM (Case *A*). (c) SCM-FJ (Case *B*). (d) DM. (e) DM-FJ (Case *C*). (f) DM-CC (Case *D*).

that any point in the feasible region can be obtained by convex combination of the four vertices. The four vertices represent four basic cases under the two taxonomies, as shown in Table I.

Case A in Fig. 2 is called *soft coupling mechanism* (SCM), which does not have parallel transmissions but n serial transmissions such as shown in Fig. 3(b). This mechanism has the minimum number of transmissions for stability, so that the actuator does not counteract the elastic force during free motion. However, it has to use bidirectional transmissions for reciprocating motion.

Case B in Fig. 2 is called *soft coupling mechanism with flexible joints* (SCM-FJ), which has n serial transmissions and n parallel transmission, as shown in Fig. 3(c). In this mechanism, the transmissions are arranged redundant so that there exists actuation force to counteract elastic force during free motion. The elastic forces can be used as restoring forces when the mechanism is implemented with unidirectional transmission. Meanwhile, the existence of the elastic internal forces limits the values of the spring stiffness, because the greater the value of the spring stiffness is, the larger actuation force is required to counteract elastic internal force during free motion.

Case C in Fig. 2 is called DM-FJ, which has m serial transmissions and n parallel transmission, as shown in Fig. 3(e). The layout of the redundant elastic springs let this mechanism appropriate for unidirectional transmissions.

Case D in Fig. 2 is called *differential mechanism with compliant couple* (DM-CC), which has m serial transmissions and $n-m$ parallel transmissions, as shown in Fig. 3(f). The layout of the minimum elastic springs does not need the actuator to counteract the elastic force in free motion but has to use bidirectional transmissions for reciprocating motion.

Note that the examples of planar two-jointed mechanisms in Fig. 3 are for explanation of the four basic cases. According to the analysis in Sections III-A and III-B, the classification method is based on the transmission mechanisms between actuators and joints and not affected by the kinematic configuration of mechanisms such as planar and spatial systems, number of joints, and shape and dimension of the structures. Although the examples in this article are tendon driven, the classification method is not affected by the mechanical forms of UCMs such as linkages and gears.

Other transmission formations can be regarded as combination of the four basic cases. For example, in the RTR II hand [45], the flexion of eight joints of three fingers is driven by an actuator via an SCM and three DM-FJs. The actuator drives three serial transmissions to flex the eight joints. Another example is the X-hand [46], where 12 joints of four fingers are driven by two actuators via an SCM and four DM-CCs. The two actuators drive four serial transmissions to flex the 12 joints. MABEL [47] utilizes the combination of a DM-CC and two CM to design a leg for walking and running.

IV. Motion and Force Analysis

Although there are different cases in UCMs, their transmission properties of motion and force can be described uniformly. In this section, we analyze the transmission properties of motion and force in joint space. To study the motion and force ability of UCMs, we introduce two subspaces of joint tangent space T_qQ and two subspaces of cotangent space T_q^*Q.

Definition 4: In a stable UCM, free joint motion under no external force is defined as *active motion*. A space spanned by all the active motion *is active motion subspace* (AMS).

Substituting $\tau = 0$ into (11), we can get

$$\Delta \mathbf{q} = -\mathbf{K}_q^{-1}\mathbf{K}_{qa}\Delta \mathbf{a} \tag{27}$$

which is a set of stable states under no external force, defining an m-dimensional submanifold in joint space, denoted as M. At

each $q \in M$, the tangent space of *M*, T_qM, is the AMS. An active motion is expressed as

$$\delta\mathbf{q}_A = -\mathbf{K}_q^{-1}\mathbf{K}_{qa}\delta\mathbf{a}. \tag{28}$$

The AMS can be expressed as the image space of $\mathbf{K}_q^{-1}\mathbf{K}_{qa}$, $\mathrm{im}(\mathbf{K}_q{}^{-1}\mathbf{K}_{qa})$. The dimension of AMS, dim(AMS), is *m*.

Definition 5: If a joint motion does not have influence on the actuator coordinates and actuation force, such joint motion is defined as *passive motion*. A space spanned by all the passive motions is *passive motion subspace* (PMS).

Substituting $\delta\mathbf{f}_a = 0$ and $\delta\mathbf{a} = 0$ into (9), we obtain

$$\mathbf{K}_{qa}^T\delta\mathbf{q} = \mathbf{0} \tag{29}$$

which is the constraint equation of passive motion. The PMS can be expressed as the kernel space of $\mathbf{K}_{qa}^T$, $\ker(\mathbf{K}_{qa}^T)$. dim(PMS) $= \dim(\ker(\mathbf{K}_{qa}^T)) = n - m$.

Definition 6: If the mechanism does not move under the control of the actuators when an external force acts on an underactuated mechanism, such an external force can be controlled and the corresponding joint torque is defined as *active force*. A space spanned by all the active forces is called *active force subspace* (AFS).

According to Definition 6, the active force is exerted by the actuators to counteract a corresponding external force that does not cause mechanical motion. Thus, an active force and its corresponding external force are actually a pair of counteracting forces. Substituting $\delta\mathbf{q} = 0$ into (8) and (9), the external force is

$$\delta\tau = \mathbf{K}_{qa}\mathbf{K}_a^{-1}\delta\mathbf{f}_a$$

whose reactive force is an active force, described as

$$\delta\tau_A = -\mathbf{K}_{qa}\mathbf{K}_a^{-1}\delta\mathbf{f}_a. \tag{30}$$

The column vectors of the matrix $\mathbf{K}_{qa}\mathbf{K}_a^{-1}$ span the AFS. dim(AFS) = dim(AMS) = *m*.

Definition 7: If an external force does not have influence on the coordinates and force of the actuators, the corresponding joint torque is defined as *passive force*. A space spanned by all the passive forces is *passive force subspace* (PFS).

Given $\delta\mathbf{a} = 0$ and $\delta\mathbf{f}_a = 0$, (7) is rewritten as

$$\mathbf{K}_{qa}^T\mathbf{K}_q^{-1}\delta\tau = \mathbf{0} \tag{31}$$

which describes the passive force. The PFS is expressed as $\ker(\mathbf{K}_{qa}^T\mathbf{K}_q^{-1})$. dim(PFS) = dim(PMS) = $n-m$.

Let $\delta V = \delta\mathbf{q}^T\mathbf{K}_q\delta\mathbf{q}$ be the change in elastic potential energy of the mechanical system [48]. It endows T_qQ with a natural Riemannian metric $\mathbf{K}_q$. Using this metric, the weighted inner product of any two points $\delta\mathbf{q}_1, \delta\mathbf{q}_2 \in T_qQ$ is defined as

$$\langle\langle\delta\mathbf{q}_1, \delta\mathbf{q}_2\rangle\rangle_{\mathbf{K}_q} = \delta\mathbf{q}_1^T\mathbf{K}_q\delta\mathbf{q}_2$$

and the orthogonal complement of T_qM can be defined as

$$T_qM^\perp = \left\{ \delta\mathbf{q}_1 \in T_qQ \middle| \langle\langle\delta\mathbf{q}_1, \delta\mathbf{q}_2\rangle\rangle_{\mathbf{K}_q} = 0 \ \ \forall\delta\mathbf{q}_2 \in T_qM \right\}. \tag{32}$$

The cotangent space T_q^*M consists of covectors that annihilate vectors in

$$T_q^*M = \left\{ \delta\tau \in T_q^*Q \middle| \langle\delta\tau, \delta\mathbf{q}\rangle = \delta\tau^T\delta\mathbf{q} = 0 \ \ \forall\delta\mathbf{q} \in T_qM^\perp \right\} \tag{33}$$

and the orthogonal complement of T_q^*M can be defined as

$$T_q^*M^\perp = \left\{ \tau \in T_q^*Q \middle| \langle\tau, \delta\mathbf{q}\rangle = 0 \ \ \forall\delta\mathbf{q} \in T_qM \right\}. \tag{34}$$

The tangent space and cotangent space can be expressed as the direct sums of their subspaces, respectively

$$T_qQ = T_qM \oplus T_qM^\perp$$
$$T_q^*Q = T_q^*M \oplus T_q^*M^\perp.$$

Take any points $\delta\mathbf{q}_A$ in AMS, $\delta\mathbf{q}_P$ in PMS, $\delta\tau_A$ in AFS, and $\delta\tau_p$ in PFS, respectively, the following equations are true:

$$\langle\langle\delta\mathbf{q}_A, \delta\mathbf{q}_P\rangle\rangle_{\mathbf{K}_q} = \left(-\mathbf{K}_q^{-1}\mathbf{K}_{qa}\delta\mathbf{a}\right)^T\mathbf{K}_q\delta\mathbf{q}_P = 0 \tag{35}$$

$$\langle\delta\tau_A, \delta\mathbf{q}_P\rangle = (-\mathbf{K}_{qa}\mathbf{K}_a^{-1}\delta\mathbf{f}_a)^T\delta\mathbf{q}_p = 0 \tag{36}$$

$$\langle\delta\tau_P, \delta\mathbf{q}_A\rangle = \delta\tau_P{}^T(-\mathbf{K}_q^{-1}\mathbf{K}_{qa}\delta\mathbf{a}) = 0$$
$$\langle\langle\delta\tau_A, \delta\tau_P\rangle\rangle_{\mathbf{K}_q^{-1}} = 0. \tag{37}$$

According to (32)–(34), the PMS is $T_qM^\perp$, the AFS is T_q^*M, and the PFS is $T_q^*M^\perp$. In conclusion, we can get the following properties.

Property 1: The motion and force spaces can split according to

$$T_qQ = \mathrm{AMS} \oplus \mathrm{PMS}$$
$$Tw_q^*Q = \mathrm{AFS} \oplus \mathrm{PFS}.$$

Property 2: AFS is the annihilator of PMS, and PFS is the annihilator of AMS.

Remark 1: According to the above two properties, the four subspaces can be divided into two groups: the first group consists of AFS and PMS, and the second group is made up of AMS and PFS. According to (29) and (30), AFS and PMS both are determined by $\mathbf{K}_{qa}$. According to (28) and (31), AMS and PFS both are determined by $-\mathbf{K}_q^{-1}\mathbf{K}_{qa}$. Thus, the two matrices determine the transmission characteristics of motion and force in any UCM.

Example 3: Analyze the four subspaces of a DM-CC in Fig. 3(f). The transmission equations of the mechanism are

$$\begin{cases} T_s = a - r_{s1}q_1 + r_{s2}q_2 \\ T_p = -r_{p1}q_1 + r_{p2}q_2 \end{cases}$$

and the system stiffness matrices are

$$\begin{cases} \mathbf{K}_q = \begin{bmatrix} k_s r_{s1}^2 + k_p {r_{p1}}^2 & k_s r_{s1} r_{s2} - k_p r_{p1} r_{p2} \\ k_s r_{s1} r_{s2} - k_p r_{p1} r_{p2} & k_s r_{s2}^2 + k_p {r_{p2}}^2 \end{bmatrix} \\ K_a = k_s \\ \mathbf{K}_{qa} = \begin{bmatrix} -k_s r_{s1} & -k_s r_{s2} \end{bmatrix}^T \end{cases}.$$

TABLE II
GROUP OF PARAMETER VALUES OF THE MECHANISM IN Fig. 3(F)

Parameters	r_{s1}	r_{s2}	r_{p1}	r_{p2}	k_s	k_p
Values	6	4	6	6	50	2.5

Unit of measurement: mm, N/mm.

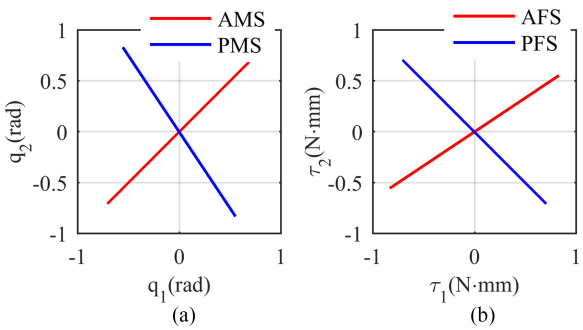

Fig. 4. (a) AMS/PMS and (b) active/passive torque subspace in the tangent space and cotangent space of joint space of the mechanism in Fig. 3(f) with the parameter values in Table II.

According to (28), the active motion equation is

$$\delta \mathbf{q}_A = \frac{r_{p1} r_{p2}}{r_{s1} r_{p2} + r_{s2} r_{p1}} \begin{bmatrix} 1/r_{p1} \\ 1/r_{p2} \end{bmatrix} \delta a.$$

The direction vector of AMS is $[1/r_{p1}\ 1/r_{p2}]^T$. According to (30), the active force equation is

$$\delta \tau_A = \begin{bmatrix} r_{s1} \\ r_{s2} \end{bmatrix} \delta f_a.$$

The direction vector of AFS is $[r_{s1}\ r_{s2}]^T$. According to (29), the passive motion is constrained in

$$\begin{bmatrix} r_{s1} & r_{s2} \end{bmatrix} \delta \mathbf{q} = 0.$$

The direction vector of PMS is $[1/r_{s1}\ -1/r_{s2}]^T$. According to (31), the passive force is constrained in

$$\begin{bmatrix} 1/r_{p1} & 1/r_{p2} \end{bmatrix} \delta \tau = 0.$$

The direction vector of PFS is $[r_{p1}\ -r_{p2}]^T$. In this mechanism, the AMS and PFS are determined by the same parameters (r_{p1}, r_{p2}), and the AFS and PMS are determined by the other parameters (r_{s1}, r_{s2}).

Given a group of parameter values of the mechanism as shown in Table II, we can get the four subspaces as shown in Fig. 4, and the corresponding four characteristic directions are shown in Table III. The $\mathbf{K}_q$-weighted inner product of AMS and AMS is zero, and the $\mathbf{K}_q{}^{-1}$-weighted inner product of AFS and AFS is zero. Meanwhile, AFS is the annihilator of PMS, and PFS is the annihilator of AMS.

The direction vectors of AMS and PMS and their annihilators determine the transmission characteristics of motion and force in a UCM. Table IV lists the direction vectors of AMS and PMS of four UCMs in Fig. 3, besides the DM-CC in Fig. 3(f).

TABLE III
FOUR CHARACTERISTIC DIRECTIONS AND JOINT STIFFNESS MATRIX

Direction vector of AMS	[1 1]	Direction vector of PMS	[2 -3]
Direction vector of AFS	[3 2]	Direction vector of PFS	[1 -1]
$\mathbf{K}_q$	$\begin{bmatrix} 1.89 & 1.11 \\ 1.11 & 0.89 \end{bmatrix} \times 10^3 N \cdot mm / rad$		

TABLE IV
DIRECTION VECTORS AND MATRIX $\mathbf{K}_q$ OF FOUR UCMS IN Fig. 3

	Direction vector of AMS	Direction vector of PMS
SCM (Fig. 3(b))	$\begin{bmatrix} \frac{1}{r_{s1}} & \frac{1}{r_{s2}} \end{bmatrix}^T$	$\begin{bmatrix} \frac{r_{s1}}{k_{s1}} & -\frac{r_{s2}}{k_{s2}} \end{bmatrix}^T$
SCM-FJ (Fig. 3(c))	$\begin{bmatrix} \frac{k_{s1}}{(k_{s1}+k_{p1})r_{s1}} & \frac{k_{s2}}{(k_{s2}+k_{p2})r_{s2}} \end{bmatrix}^T$	$\begin{bmatrix} \frac{r_{s1}}{k_{s1}} & -\frac{r_{s2}}{k_{s2}} \end{bmatrix}^T$
DM-FJ (Fig. 3(e))	$\begin{bmatrix} \frac{r_{s2}}{k_{p1}} & \frac{r_{s2}}{k_{p2}} \end{bmatrix}^T$	$\begin{bmatrix} \frac{1}{r_{s1}} & -\frac{1}{r_{s2}} \end{bmatrix}^T$
DM-CC (Fig. 3(f))	$\begin{bmatrix} \frac{1}{r_{p1}} & \frac{1}{r_{p2}} \end{bmatrix}^T$	$\begin{bmatrix} \frac{1}{r_{s1}} & -\frac{1}{r_{s2}} \end{bmatrix}^T$

V. TRANSMISSION PRINCIPLE OF UCMS

In this section, we establish a relationship between mechanical structure and function based on the classification and the transmission properties of UCMs. It will be used to guide the design in the following section.

A. Transmission Principle in UCMs

According to the previous analysis of force and motion in UCMs, two classes of relationships can be summarized as follows.

1) Annihilator Relation: According to Property 2, AFS is the annihilator of PMS. It means that if any one of them is known, the other is known. AFS and PMS both are characterized by the matrix $\mathbf{K}_{qa}$. Likewise, AMS is the annihilator of PFS, and both are characterized by the matrix $\mathbf{K}_q^{-1}\mathbf{K}_{qa}$.

2) Dual Relation: AFS is a dual space of AMS. The active force is related to the active motion through the stiffness matrix $\mathbf{K}_q$ as follows:

$$\delta \tau_A = -\mathbf{K}_q \delta \mathbf{q}_A.$$

It means that the relative direction of active motion and active force is closely related to the stiffness matrix. Similarly

$$\delta \tau_P = -\mathbf{K}_q \delta \mathbf{q}_P.$$

The dual relation is characterized by the stiffness matrix $\mathbf{K}_q$. According to (35), PMS is orthogonal to AMS under the metric $\mathbf{K}_q$. Meanwhile, the positive definiteness of $\mathbf{K}_q$ is the basis for judging the stability of UCMs.

To sum up, we can conclude three characteristics of compliant underactuated transmission as follows:

1) the stability: characterized by the joint stiffness matrix $\mathbf{K}_q$;
2) the transmission of active motion and passive force: characterized by the column vectors of $\mathbf{K}_{qa}$;

3) the transmission of active force and passive motion: characterized by the column vectors of $\mathbf{K}_q^{-1}\mathbf{K}_{qa}$.

The three characteristics are determined by the mechanical structure and its geometric and elastic parameters. We are particularly concerned with characteristics determined completely by geometric parameters. It is because the geometric parameters are only affected by the position deviation, more reliable than the elastic parameters that are affected by the deviations of both position and force. The characteristic only determined by the geometric parameters is called *GP-based characteristics*.

In addition to these three characteristics, there is another characteristic that is

4) the redundancy of the transmission. It is characterized by the actuation force during free motion, and determined by the number of independent transmissions.

A mechanism with minimum number of transmissions for stabilization means that the actuators do not counteract the elastic force in free motion. Note that this mechanism has to use bidirectional transmissions for reciprocating motion. Compared with bidirectional transmissions, unidirectional transmission usually has lower cost of building and needs redundant transmissions to provide restoring forces.

The four characteristics correlate the mechanical structure to the function of motion and force in UCMs. The relationship between mechanical structure and function of different cases is shown in the following section.

B. Structure and Function in Different Cases

This section investigates different cases of UCMs with the previous four transmission characteristics to establish the relationship of structure and function. We are focused on the four cases of UCMs introduced in Section III. Each case of the underactuated mechanisms can be implemented with different transmission styles such as linkage, gears, and tendon pulley. Here, we use pulley-tendon one-actuator three-jointed mechanisms as examples to illustrate the four cases.

As the four transmission characteristics for each example, the joint stiffness matrix, the actuation force for free motion, the directions of active motion and active torque are derived according to (10), (28), (30), and (17), and given in Table V. Because both the number and the layout of transmissions are different during the four cases, the characteristic parameters also are significantly different, as shown in Table V. The particularity of the four cases is induced as follows.

1) Soft Coupling Mechanism: This mechanism has minimum number of transmissions for stabilization, so that the actuator does not counteract the elastic force in free motion. However, this mechanism has to use bidirectional transmissions for reciprocating motion.

The direction of active motion, $[\,1/r_{s1}\ 1/r_{s2}\ 1/r_{s3}\,]^T$, is only determined by the geometric parameters. This property let the SCM apply in the occasion needing reliable active motion, such as flapping-wing flighting [7] and humanlike natural motion for rehabilitation [49].

The direction of active force, $[\,k_{s1}/r_{s1}\ k_{s2}/r_{s2}\ k_{s3}/r_{s3}\,]^T$, is related with both the radii of pulleys and the stiffness of springs. It means that the load capacity depends heavily on spring stiffness. However, the spring stiffness is related with the system compliance. Hence, the selection of spring stiffness should tradeoff the system compliance and active force ability.

Note that the pulley parameter $r_{si} \in \Re$ contains information about the routing direction of rope and the radius of pulley according to Example 1. Since the stiffness values of the springs are positive, the active force has the same sign as the active motion on each joint. Hence, in this mechanism, active motion and active force could not be *regulated independently*.

2) Soft Coupling Mechanism With Flexible Joints: The direction of active force

$$\left[\ \frac{k_{s1}}{(k_{s1}+k_{p1})r_{s1}}\ \ \frac{k_{s2}}{(k_{s2}+k_{p2})r_{s2}}\ \ \frac{k_{s3}}{(k_{s3}+k_{p3})r_{s3}}\ \right]^T$$

and the direction of active motion $[\,k_{s1}/r_{s1}\ k_{s2}/r_{s2}\ k_{s3}/r_{s3}\,]^T$ both are related with the radii of pulleys and the stiffness of springs, and consistent on the corresponding joint. Meanwhile, the active force has the same sign as the active motion on each joint. The SCM-FJ has the same characteristics as fluidic actuated soft robots such as pneu-net design [50] and fiber-reinforced soft actuators [51].

The redundant layout of the transmissions lets this mechanism appropriate for unidirectional transmissions, but leads to actuation force that counteracts the elastic force in free motion. Usually, the cost of building such underactuated robots is significantly low [16]. However, it is a problem to be overcome that is to reduce the energy consumption in the self-bending process of the mechanism [51].

3) Differential Mechanism With Flexible Joints: The direction of active force, $[\,r_{s1}\ r_{s2}\ r_{s3}\,]^T$, is determined only by the geometric parameters so that the DM apply in the occasion where specific joint torque distribution is maintained, such as adaptively holding on objects of different shape [23].

The direction of active motion, $[\,r_{s1}/k_{p1}\ r_{s2}/k_{p2}\ r_{s3}/k_{p3}\,]^T$, related with both the radii of pulleys and the spring stiffness, is the same sign as the active force on each joint.

This mechanism with redundant layout of transmissions appropriates for unidirectional transmissions and has significantly low cost of building. Hence, the DM-FJ was used in robot and prosthetic hands [14], [15]. Meanwhile, the selection of spring stiffness must take the energy consumption and active motion trajectory into account.

4) Differential Mechanism With Compliant Couple: The direction of active motion, $[\,1/r_{p1}\ 1/r_{p2}\ 1/r_{p3}\,]^T$, and the direction of active force, $[\,r_{s1}\ r_{s2}\ r_{s3}\,]^T$, are regulated by two separate groups of geometric parameters, respectively. Hence, the directions of active motion and active force can be regulated completely independently.

In the DM-CC, the active force is exerted by the serial transmission, and the passive force is provided by the parallel transmissions. The directions of active motion and active force are unaffected by stiffness. Thus, the regulation of stiffness is nothing to do with the directions of motion and force.

The minimal number of transmissions induces that this mechanism has to use bidirectional transmissions for reciprocating motion. However, it does not need to counteract the elastic force

TABLE V
FOUR CASES OF STABLE UNDERACTUATED MECHANISMS IN A THREE-JOINTED FINGER

Case	SCM	SCM-FJ	DM-FJ	DM-CC
Example	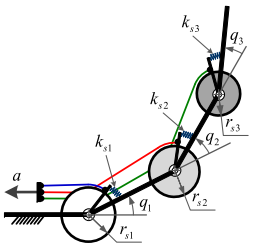	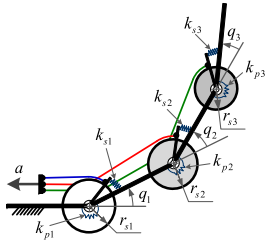	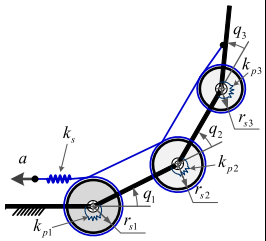	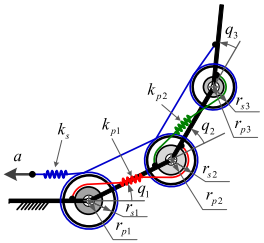
Transmission	$\mathbf{T}_s = \begin{bmatrix} a/r_{s1} - q_1 \\ a/r_{s2} - q_2 \\ a/r_{s3} - q_3 \end{bmatrix}$	$\mathbf{T}_s = \begin{bmatrix} a/r_{s1} - q_1 \\ a/r_{s2} - q_2 \\ a/r_{s3} - q_3 \end{bmatrix}$, $\mathbf{T}_p = \begin{bmatrix} q_1 \\ q_2 \\ q_3 \end{bmatrix}$	$T_s = a - r_{s1}q_1 - r_{s2}q_2 - r_{s3}q_3$ $\mathbf{T}_p = \begin{bmatrix} q_1 & q_2 & q_3 \end{bmatrix}^T$	$T_s = a - r_{s1}q_1 - r_{s2}q_2 - r_{s3}q_3$ $\mathbf{T}_p = \begin{bmatrix} r_{p2}q_2 - r_{p1}q_1 \\ r_{p3}q_3 - r_{p2}q_2 \end{bmatrix}$
Joint stiffness matrix $\mathbf{K}_q$	$\begin{bmatrix} k_{s1} & 0 & 0 \\ 0 & k_{s2} & 0 \\ 0 & 0 & k_{s3} \end{bmatrix}$	$\begin{bmatrix} k_{s1}+k_{p1} & 0 & 0 \\ 0 & k_{s2}+k_{p2} & 0 \\ 0 & 0 & k_{s3}+k_{p3} \end{bmatrix}$	$\begin{bmatrix} k_{p1}+k_s r_{s1}^2 & k_s r_{s1} r_{s2} & k_s r_{s1} r_{s3} \\ k_s r_{s1} r_{s2} & k_{p2}+k_s r_{s2}^2 & k_s r_{s2} r_{s3} \\ k_s r_{s1} r_{s3} & k_s r_{s2} r_{s3} & k_{p3}+k_s r_{s3}^2 \end{bmatrix}$	$\begin{bmatrix} k_s r_{s1}^2 + k_{p1} r_{p1}^2 & k_s r_{s1} r_{s2} - k_{p1} r_{p1} r_{p2} & k_s r_{s1} r_{s3} \\ k_s r_{s1} r_{s2} - k_{p1} r_{p1} r_{p2} & k_s r_{s2}^2 + k_{p1} r_{p2}^2 + k_{p2} r_{p2}^2 & k_s r_{s2} r_{s3} - k_{p2} r_{p2} r_{p3} \\ k_s r_{s1} r_{s3} & k_s r_{s2} r_{s3} - k_{p2} r_{p2} r_{p3} & k_s r_{s3}^2 + k_{p2} r_{p3}^2 \end{bmatrix}$
Actuation force during free motion	0	$f_a = -\left(\frac{k_{s1}k_{p1}}{(k_{s1}+k_{p1})r_{s1}^2} + \frac{k_{s2}k_{p2}}{(k_{s2}+k_{p2})r_{s2}^2} + \frac{k_{s3}k_{p3}}{(k_{s3}+k_{p3})r_{s3}^2} \right) \Delta a$	$f_a = -\frac{\Delta a}{r_{s1}^2/k_{p1} + r_{s2}^2/k_{p2} + r_{s3}^2/k_{p3} + 1/k_s}$	0
Direction of Active motion	$\begin{bmatrix} 1/r_{s1} & 1/r_{s2} & 1/r_{s3} \end{bmatrix}^T$	$\begin{bmatrix} \frac{k_{s1}}{(k_{s1}+k_{p1})r_{s1}} & \frac{k_{s2}}{(k_{s2}+k_{p2})r_{s2}} & \frac{k_{s3}}{(k_{s3}+k_{p3})r_{s3}} \end{bmatrix}^T$	$\begin{bmatrix} r_{s1}/k_{p1} & r_{s2}/k_{p2} & r_{s3}/k_{p3} \end{bmatrix}^T$	$\begin{bmatrix} 1/r_{p1} & 1/r_{p2} & 1/r_{p3} \end{bmatrix}$
Direction of Active force	$\begin{bmatrix} k_{s1}/r_{s1} & k_{s2}/r_{s2} & k_{s3}/r_{s3} \end{bmatrix}^T$	$\begin{bmatrix} k_{s1}/r_{s1} & k_{s2}/r_{s2} & k_{s3}/r_{s3} \end{bmatrix}^T$	$\begin{bmatrix} r_{s1} & r_{s2} & r_{s3} \end{bmatrix}^T$	$\begin{bmatrix} r_{s1} & r_{s2} & r_{s3} \end{bmatrix}^T$
Characteristics	– Bidirectional transmissions – GP-based transmission of active motion	– Unidirectional or bidirectional transmission	– Unidirectional or bidirectional transmission – GP-based transmission of active force	– Bidirectional transmissions – GP-based transmission of active motion – GP-based transmission of active force – Independent regulation of active motion and active force

Note that in the first two figures the obscured routings at the first and the second joint are through the corresponding axles.

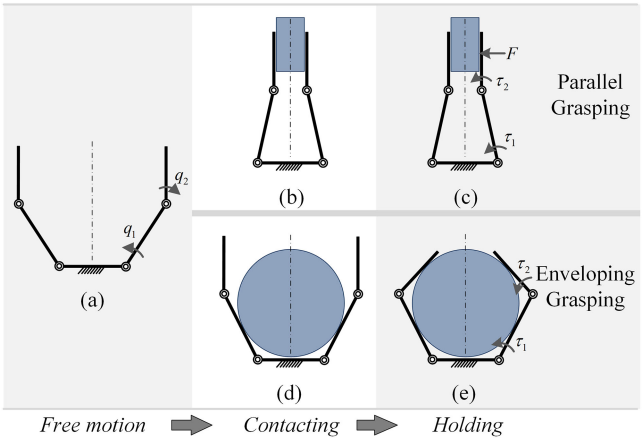

Fig. 5. Functional requirement of parallel grasp and enveloping grasp.

in free motion. Hence, the DM-CC has low energy consumption and good energy efficiency.

VI. Functional Oriented Design and Implementation of a Two-Fingered Gripper

This section uses the previous theory to design a simple and practical single-actuator hand to achieve envelope and precision grasps. Underactuated hands are adept at adaptively grasping objects of different shape and size [23], whereas its precision grasping ability is limited [17] because of the existence of uncontrollable contact forces and movements. Usually, it is very hard to design a versatile single-actuator robot hand [52].

Consider a one-actuator two-fingered gripper, where each finger has two joints. An effective way to achieve envelope and precision grasps with underactuated hands is: 1) to use the passive adaptiveness to achieve envelope grasp, and 2) to use fingertip parallel motion to achieve precision grasp. The core problem is to ensure the active parallel movement of the two distal phalanges while the active force of the gripper applied onto the grasped object. During precision grasping, to ensure that the two fingers are always parallel during the movement from open to closed, the active movement signs of the proximal and distal joints must be opposite, as shown in Fig. 5(a) and (b). The distal phalanx should actively apply force onto the object after it is in contact with the object. Hence, the active force has the same signs in the proximal and distal joints, as shown in Fig. 5(c). In enveloping grasping, after the proximal phalanx is in contact with the object, the distal joint change the movement direction to adapt to the object, as shown in Fig. 5(d) and (e).

According to the above analysis of functional requirement, two transmission characteristics are summarized as follows.

1) In order to keep the two distal phalanges parallel during free motion, the two joints of each finger move in opposite directions.
2) In each finger, the active forces of the two joints are in the same direction to squeeze the grasped object.

To sum up, in each finger, the active motion and the active force have the same sign on proximal joint but different sign on distal joint.

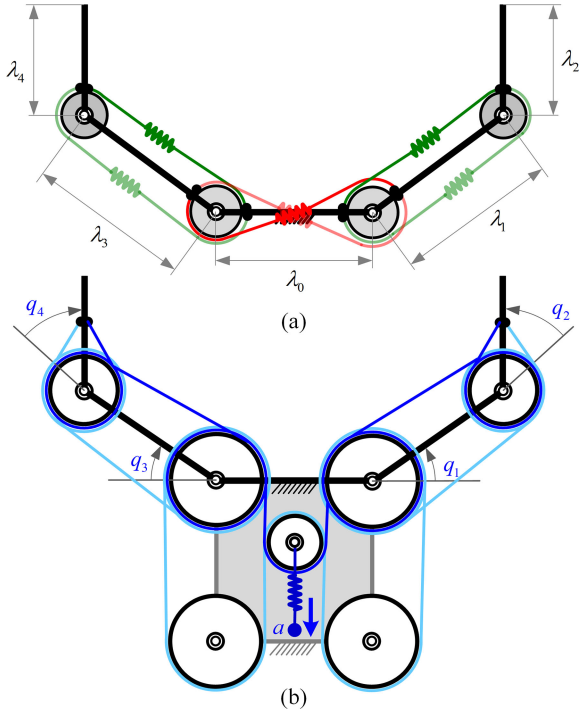

Fig. 6. DM-CC is constituted by (a) three groups of parallel transmissions and (b) a group of serial transmission.

To design a transmission mechanism meeting the above requirements, the six underactuated mechanisms in Fig. 3 are alternatives. The DM in Fig. 3(d) cannot meet the requirement of the stable movement before contacting to the grasped objects. The CM in Fig. 3(a) cannot meet the requirement of the adaptive enveloping after the proximal phalanx contacts to the objects. The other four underactuated mechanisms in Fig. 3, namely the four cases of UCMs, all have the ability to move stably and to grasp adaptively.

According to the relationship between the mechanical structure and transmission function of the UCMs in Section V-B, the active motion and the active force have the same sign on each joint of the SCM, SCM-FJ, and DM-FJ. Thus, the three cases of UCMs cannot meet the functional requirement as shown in Fig. 5, where the active motion and active force have the same sign on proximal joint but different signs on distal joint. In the last case of UCMs, namely DM-CC, the active motion and active force are regulated by two separate groups of geometric parameters, respectively. Thus, the DM-CC can meet the requirements in Fig. 5.

A one-actuator four-jointed gripper is designed with a DM-CC and implemented with tendon-pulley mechanisms. Its transmissions are arranged as follows.

1) In order to satisfy the reverse movement of the proximal and distal joints in each finger, the two joints of a finger are coupled by a pair of transmission in the same direction, as green lines in Fig. 6(a).
2) In order to move the two fingers toward each other in opposite directions, the two proximal joints are coupled by a parallel transmission, as red lines in Fig. 6(a).

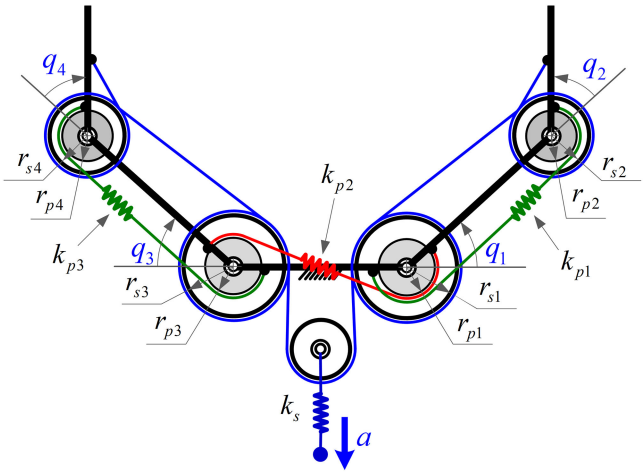

Fig. 7. Schematic diagram of two-fingered gripper driven by a single actuator.

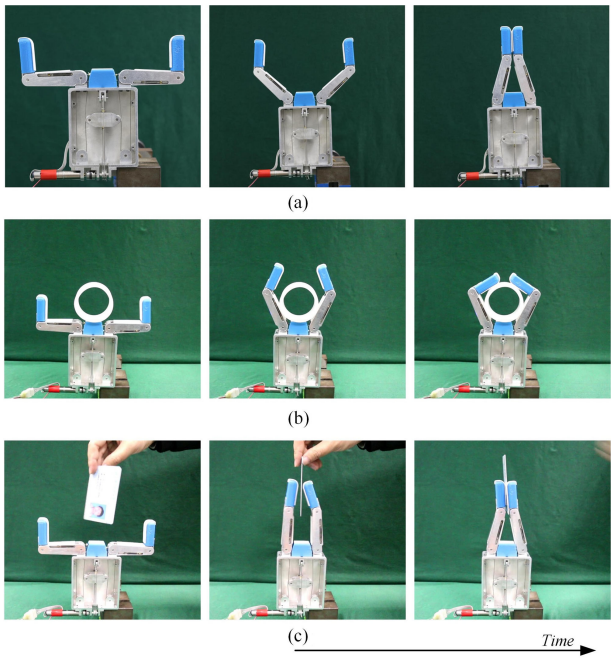

Fig. 8. Close sequences of a one-actuator two-fingered prototype gripper. (a) Free moving. (b) Envelope grasping. (c) Parallel grasping.

TABLE VI
PARAMETER VALUES OF THE PROTOTYPE GRASPER

Parameters	λ_0	$\lambda_{1,3}$	$\lambda_{2,4}$	$r_{s1,3}$	$r_{s2,4}$	$r_{p1,2,3,4}$	k_s	$k_{p1,2,3}$
Values	40	60	40	7	4	6	40	2.5

Unit of measurement: mm, N/mm.

3) In order to ensure that fingers actively exert force on the grasped object, we use a serial transmission to connect the four joints differentially as in Fig. 6(b).

According to the above design of transmissions, the schematic diagram of the gripper can be given in Fig. 7. Its structure and parameters are labeled in Figs. 6 and 7. The gripper has a serial transmission and three parallel transmissions, expressed as

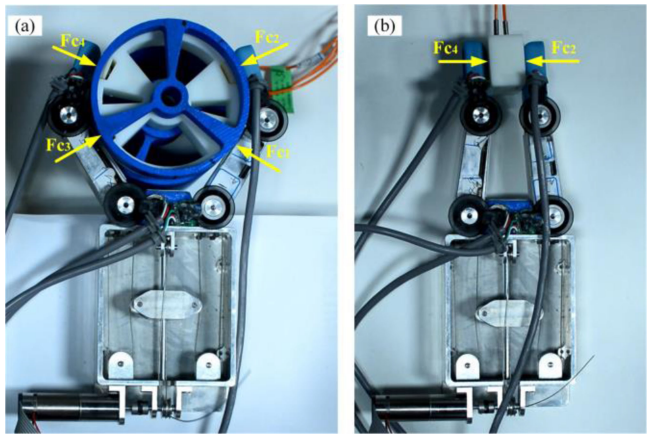

Fig. 9. Experimental setup. (a) Enveloping grasp. (b) Parallel grasp.

$$\begin{cases} T_s = a - (r_{s1}q_1 + r_{s2}q_2 + r_{s3}q_3 + r_{s4}q_4)/2 \\ T_{p1} = r_{p1}q_1 + r_{p2}q_2 \\ T_{p2} = r_{p1}q_1 - r_{p3}q_3 \\ T_{p3} = r_{p3}q_3 + r_{p4}q_4 \end{cases}.$$

The transmission Jacobian matrices are

$$\mathbf{J}_{s1} = -\frac{1}{2}\begin{bmatrix} r_{s1} & r_{s2} & r_{s3} & r_{s4} \end{bmatrix}$$

$$\mathbf{J}_{s2} = 1$$

$$\mathbf{J}_p = \begin{bmatrix} r_{p1} & r_{p2} & 0 & 0 \\ r_{p1} & 0 & -r_{p3} & 0 \\ 0 & 0 & r_{p3} & r_{p4} \end{bmatrix}.$$

The stiffnesses of serial and parallel springs are

$$\mathbf{K}_s = k_a$$

$$\mathbf{K}_p = \mathrm{diag}(k_{p1}, k_{p2}, k_{p3}).$$

According to (28), the direction of the active motion is

$$\begin{bmatrix} 1/r_{p1} & -1/r_{p2} & 1/r_{p3} & -1/r_{p4} \end{bmatrix}^T.$$

When

$$r_{p1} = r_{p2} = r_{p3} = r_{p4}$$

the direction of the active motion is

$$\begin{bmatrix} 1 & -1 & 1 & -1 \end{bmatrix}^T$$

then the two joints of each finger rotate reversely at the same speed, and the two fingers move symmetrically. Thus, the two distal phalanges of the gripper can keep parallel during the free motion.

According to (30), the direction of the active force is

$$\begin{bmatrix} r_{s1} & r_{s2} & r_{s3} & r_{s4} \end{bmatrix}^T$$

which guarantee the active forces to squeeze the grasped object in either enveloping grasp or precision grasp.

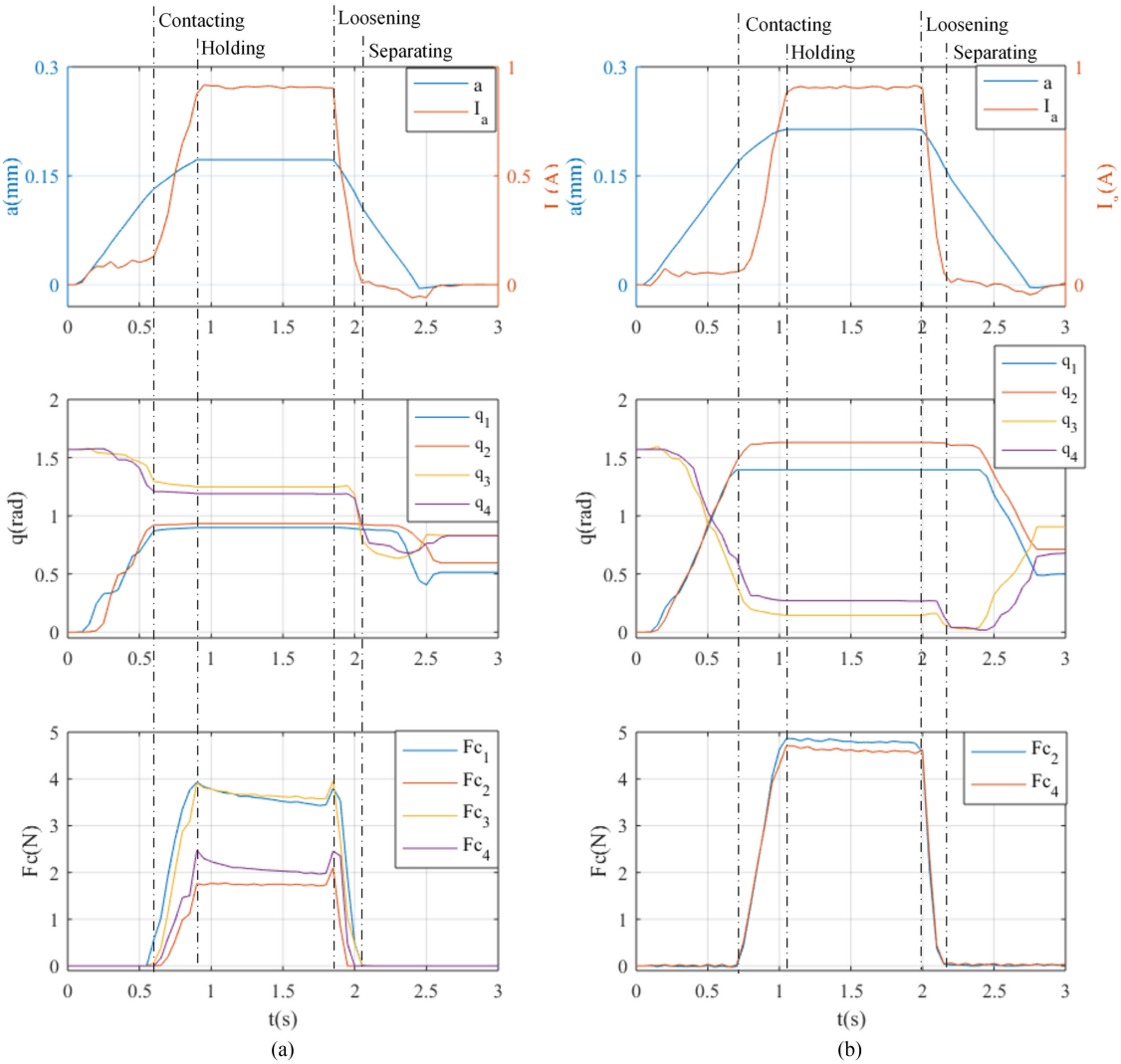

Fig. 10. Measured experimental results. (a) Enveloping grasping a cylinder of $r = 45$ mm. (b) Parallel grasping a brick with a thickness of 20 mm.

Consider the convergence of adaptive grasping [2], a group of feasible parameter values is given as

$$r_{s1}/r_{s2} = r_{s3}/r_{s4} = 2$$

then the direction of the active force is

$$\begin{bmatrix} 2 & 1 & 2 & 1 \end{bmatrix}^T.$$

Based on the analysis results, a prototype gripper shown in Fig. 8 was built with the same kinematics as the transmission mechanism shown as Fig. 7. According to the above analysis, the mechanism parameter values of the prototype gripper are chosen in Table VI. Note that k_s is the stiffness of the driven tendon (Cable 2019-SN, Carl Stahl Sava Industries, Inc., namely Bowden cable, 0.6-mm nylon-coated steel cable). This gripper is driven by a dc motor via the tendon.

Fig. 8 shows the closing sequence of the prototype gripper driven by the motor. During free moving, constrained by the three parallel transmissions in Fig. 6(a), the proximal links bend and distal links stretch so that the two distal links keep parallel from open to close as in Fig. 8(a). During enveloping grasping a cylinder, when the proximal links contact with the cylinder, the motion of proximal joints is restricted, whereas the distal joints are bending, as shown in Fig. 8(b). After the distal joints contact with it, the cylinder is squeezed by all the four links under the active transmission. Thus, the cylinder is enveloped firmly. During parallel grasping a card, the distal links clamp parallelly and squeeze the card after contacting, as shown in Fig. 8(c). Note that the two distal links are not completely parallel before grasping, as shown in the middle status of the parallel grasping in Fig. 8(c). This deviation between practice and theory is due to friction and gravity. It does not have a significant impact on grasping effect. The grasping processes shown in Fig. 8 exhibit the aforementioned desired characteristics to achieve enveloping grasp and precision grasp.

The grasping scenario in Fig. 5 is replicated in experiments to measure the grasping trajectories and the contact forces, as shown in Fig. 9. The gripper is fixed on a table and the grasped objects are free within the grasping scope so that the objects can freely move on the table as the gripper grasps. The gripper is driven with a constant speed of $v = 0.25$ mm·s^{-1} by the

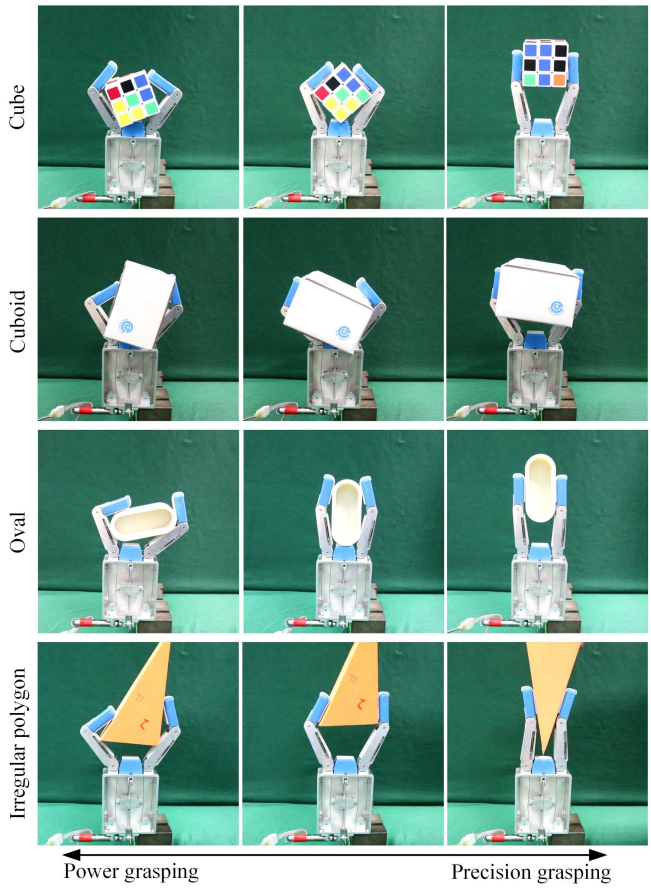

Fig. 11. Examples of grasping executed with the prototype gripper. The shape of the grasped object in each row is different, which is a cube, a cuboid, an oval, and an irregular polygon.

dc motor (Maxon DCX16S, gear GPX16 44:1, and encoder ENX16) and a guide bar. The maximum current of the motor is set to 0.9 A. Optical encoders with 1024 counts/revolution are used to measure the joint angles. Four pressure sensors with 1/20 N resolution are mounted on the grasped objects to record the contact forces on the contact with phalanges. The force and position are measured at a sample frequency of 20 Hz. All experiments were repeated three times, and the force and position were averaged over the three trials.

Fig. 10 shows the experiment results of the actuator current I_a, actuator coordinate, joint trajectories, and contact forces during the grasping process in (a) enveloping grasping a cylinder of $r = 45$ mm and (b) parallel grasping a brick with a thickness of 20 mm. Both in the enveloping and parallel grasps, there are obviously five stages, namely free motion, contacting, holding, loosening, and separating. During the free motion, with the increase of actuator displacement, the motor current always fluctuates near a low value ($I_a = 0.08$ A) and the joints are basically moving at a constant speed. The nonlinear part of joint motion is due in large part to the friction within the transmission mechanism from the motor to the joints, which is verified by the low current generated in working against resistance in the transmission mechanism. After the fingers contact the grasped object, with the increase the motor current, the actuator, and joints decelerate and the contact forces increase from zero. After the current reaches the threshold ($I_a = 0.9$ A), the actuator and joints are not moving anymore, but the current and contact forces fluctuate slightly. It means that the objects have been held firmly. The complete experimental process can be seen in the supplementary material.

Fig. 11 exhibits the prototype gripper grasping objects of different shapes using different grasping patterns. The experimental results show that the robot gripper has good shape self-adaptability and fingertip grasping ability for objects different shapes. The complete grasping processes can be seen in the supplementary material.

To our knowledge, there were two grippers that can realize parallel grasping and enveloping grasping. One is a linkage two-fingered gripper Robotiq 2F-85[1], and the other is a tendon-driven two-fingered gripper Velo [52]. This Robotiq 2F-85 gripper is carried out by a linkage mechanism so that the proximal phalanx is very thick. Through experience design of mechanical structure and optimization of parameters, the Velo gripper used complicated routing of the active/passive tendons and the meticulous arrangement of elastic elements. In our proposed gripper, through the analysis and comparison of different transmission mechanisms, a simple and compact design scheme is proposed and adopted. In the designed gripper, a tendon-driven DM-CC is first used for parallel and enveloping grasps. The experimental results show that the proposed gripper realizes the original design target.

VII. Conclusion

To analyze and design the transmission structure of UCMs, in this article we classified systematically the UCMs and revealed the active and passive transmission properties of force and motion in UCMs. Combining the transmission properties of motion and force, this new taxonomy can distinguish significantly different cases of UCMs from both mechanical structure and transmission function. Synthesizing the classification and the transmission properties of UCMs, the congruent relationship between mechanical structure and transmission function was established from the four aspects, namely stability, redundancy of transmission chains, transfer characteristics of active force and active motion. Based on the relationship between structure and functions in UCMs, a function-oriented design method was proposed. We used the proposed method to design a single-actuator two-fingered gripper achieving envelope and precision grasps. The results showed that a versatile single-actuator gripper can be implemented through a simple design of the transmission structure.

We also analyzed and compared different cases of UCMs, and demonstrated that the DM-CC has excellent transmission characteristics, namely minimum number of transmissions, GP-based transmissions of active motion and active force, independent regulation of passive stiffness, active motion, and active force. In a word, the DM-CC decouples the active and passive transmissions of force and motion. We used the DM-CC in

[1][Online]. Available: http://www.robotiq.com

the designed versatile single-actuator gripper and demonstrated its adaptive enveloping and precision grasping function that is difficult to achieve with other cases of UCMs.

In this article, we focused on the transmission structure of UCMs. Different from the equilibrium force analysis [21], [43], we proposed the analysis and design methodology of UCMs based on the relationship between the mechanical structure of serial and parallel compliance and the active and passive transmission properties of force and motion. The proposed methodology provided a new perspective to understand and design UCMs through deconstructing the active and passive transmissions of force and motion. Further research will expand the methodology into the design of UCMs for specific applications such as dexterous grasping and manipulation. In contrast, we do not treat some problems that were considered optimization of the mechanism parameters for grasp qualities. It will further improve the performance of UCMs.

REFERENCES

[1] C. Gosselin, "Adaptive robotic mechanical systems: A design paradigm," *J. Mech. Des.*, vol. 128, no. 1, pp. 192–198, 2006.

[2] W. Chen, C. Xiong, W. Chen, and S. Yue, "Mechanical adaptability analysis of underactuated mechanisms," *Robot. Comput.-Integr. Manuf.*, vol. 49, pp. 436–447, 2018.

[3] A. Bicchi, M. Gabiccini, and M. Santello, "Modelling natural and artificial hands with synergies," *Philos. Trans. Roy. Soc. London B Biol. Sci.*, vol. 366, no. 1581, pp. 3153–3161, 2011.

[4] J. Buchli and A. J. Ijspeert, "Self-organized adaptive legged locomotion in a compliant quadruped robot," *Auton. Robots*, vol. 25, no. 4, pp. 331–347, 2008.

[5] S. Kim, M. Spenko, S. Trujillo, B. Heyneman, D. Santos, and M. R. Cutkosky, "Smooth vertical surface climbing with directional adhesion," *IEEE Trans. Robot.*, vol. 24, no. 1, pp. 65–74, Feb. 2008.

[6] A. D. Ames, "First steps toward underactuated human-inspired bipedal robotic walking," in *Proc. IEEE Int. Conf. Robot. Autom.*, Saint Paul, MN, USA, 2012, pp. 1011–1017.

[7] R. J. Wood, "The first takeoff of a biologically inspired at-scale robotic insect," *IEEE Trans. Robot.*, vol. 24, no. 2, pp. 341–347, Apr. 2008.

[8] P. S. Sreetharan and R. J. Wood, "Passive torque regulation in an underactuated flapping wing robotic insect," *Auton. Robots*, vol. 31, no. 2/3, pp. 225–234, 2011.

[9] A. Ramezani, S.-J. Chung, and S. Hutchinson, "A biomimetic robotic platform to study flight specializations of bats," *Sci. Robot.*, vol. 2, no. 3, 2017, Art. no. eaal2505.

[10] A. Chiri, N. Vitiello, F. Giovacchini, S. Roccella, F. Vecchi, and M. C. Carrozza, "Mechatronic design and characterization of the index finger module of a hand exoskeleton for post-stroke rehabilitation," *IEEE/ASME Trans. Mechatron.*, vol. 17, no. 5, pp. 884–894, Oct. 2012.

[11] A. Battezzato, "Towards an underactuated finger exoskeleton: An optimization process of a two-phalange device based on kinetostatic analysis," *Mechanism Mach. Theory*, vol. 78, pp. 116–130, 2014.

[12] J. Iqbal, H. Khan, N. G. Tsagarakis, and D. G. Caldwell, "A novel exoskeleton robotic system for hand rehabilitation—Conceptualization to prototyping," *Biocybern. Biomed. Eng.*, vol. 34, no. 2, pp. 79–89, 2014.

[13] T. Laliberté and C. M. Gosselin, "Simulation and design of underactuated mechanical hands," *Mechanism Mach. Theory*, vol. 33, no. 1, pp. 39–57, 1998.

[14] A. M. Dollar and R. D. Howe, "The highly adaptive SDM hand: Design and performance evaluation," *Int. J. Robot. Res.*, vol. 29, no. 5, pp. 585–597, 2010.

[15] C. Cipriani, M. Controzzi, and M. C. Carrozza, "The SmartHand transradial prosthesis," *J. NeuroEng. Rehabil.*, vol. 8, 2011, Art. no. 29.

[16] R. Deimel and O. Brock, "A novel type of compliant and underactuated robotic hand for dexterous grasping," *Int. J. Robot. Res.*, vol. 35, no. 1–3, pp. 161–185, 2016.

[17] G. Kragten, M. Baril, C. Gosselin, and J. Herder, "Stable precision grasps by underactuated grippers," *IEEE Trans. Robot.*, vol. 27, no. 6, pp. 1056–1066, Dec. 2011.

[18] L. U. Odhner and A. M. Dollar, "Stable, open-loop precision manipulation with underactuated hands," *Int. J. Robot. Res.*, vol. 34, no. 11, pp. 1347–1360, 2015.

[19] D. Prattichizzo, M. Malvezzi, M. Gabiccini, and A. Bicchi, "On motion and force controllability of precision grasps with hands actuated by soft synergies," *IEEE Trans. Robot.*, vol. 29, no. 6, pp. 1440–1456, Dec. 2013.

[20] L. Birglen and C. M. Gosselin, "On the force capability of underactuated fingers," in *Proc. IEEE Int. Conf. Robot. Autom.*, Taipei, China, 2003, vol. 1, pp. 1139–1145.

[21] L. Birglen and C. M. Gosselin, "Kinetostatic analysis of underactuated fingers," *IEEE Trans. Robot. Autom.*, vol. 20, no. 2, pp. 211–221, Apr. 2004.

[22] A. M. Dollar and R. D. Howe, "Joint coupling design of underactuated hands for unstructured environments," *Int. J. Robot. Res.*, vol. 30, no. 9, pp. 1157–1169, 2011.

[23] L. Birglen, T. Laliberté, and C. M. Gosselin, *Underactuated Robotic Hands* (Springer Tracts in Advanced Robotics). Berlin, Germany: Springer-Verlag, 2008.

[24] F. Iida, "Cheap design approach to adaptive behavior: Walking and sensing through body dynamics," in *Proc. Int. Symp. Adapt. Motion Animals Mach.*, 2005, p. 15.

[25] A. M. Dollar and R. D. Howe, "Joint coupling design of underactuated grippers," in *Proc. ASME Int. Des. Eng. Tech. Conf. Comput. Inf. Eng. Conf.*, 2006, vol. 2006, pp. 903–911.

[26] M. Santello *et al.*, "Hand synergies: Integration of robotics and neuroscience for understanding the control of biological and artificial hands," *Phys. Life Rev.*, vol. 17, pp. 1–23, 2016.

[27] S. Hirose and Y. Umetani, "The development of soft gripper for the versatile robot hand," *Mechanism Mach. Theory*, vol. 13, no. 3, pp. 351–359, 1978.

[28] R. Ozawa, Y. Mishima, and Y. Hirano, "Design of a transmission with gear trains for underactuated mechanisms," *IEEE Trans. Robot.*, vol. 32, no. 6, pp. 1399–1407, Dec. 2016.

[29] K. Xu and H. Liu, "Continuum differential mechanisms and their applications in gripper designs," *IEEE Trans. Robot.*, vol. 32, no. 3, pp. 754–762, Jun. 2016.

[30] M. Santello, M. Flanders, and J. F. Soechting, "Postural hand synergies for tool use," *J. Neurosci.*, vol. 18, no. 23, pp. 10105–10115, 1998.

[31] I. V. Grinyagin, E. V. Biryukova, and M. A. Maier, "Kinematic and dynamic synergies of human precision-grip movements," *J. Neurophysiol.*, vol. 94, no. 4, pp. 2284–2294, 2005.

[32] M. Santello, G. Baud-Bovy, and H. Jörntell, "Neural bases of hand synergies," *Frontiers Comput. Neurosci.*, vol. 7, no. 7, pp. 2301–2315, 2013.

[33] C. Y. Brown and H. H. Asada, "Inter-finger coordination and postural synergies in robot hands via mechanical implementation of principal components analysis," in *Proc. IEEE/RSJ Int. Conf. Intell. Robots Syst.*, San Diego, CA, USA, 2007, pp. 2877–2882.

[34] W. Chen, C. Xiong, and S. Yue, "Mechanical implementation of kinematic synergy for continual grasping generation of anthropomorphic hand," *IEEE/ASME Trans. Mechatron.*, vol. 20, no. 3, pp. 1249–1263, Jun. 2015.

[35] M. G. Catalano, G. Grioli, E. Farnioli, A. Serio, C. Piazza, and A. Bicchi, "Adaptive synergies for the design and control of the Pisa/IIT SoftHand," *Int. J. Robot. Res.*, vol. 33, no. 5, pp. 768–782, 2014.

[36] M. Gabiccini, A. Bicchi, D. Prattichizzo, and M. Malvezzi, "On the role of hand synergies in the optimal choice of grasping forces," *Auton. Robots*, vol. 31, no. 2, pp. 235–252, 2011.

[37] G. A. Pratt and M. M. Williamson, "Series elastic actuators," in *Proc. IEEE/RSJ Int. Conf. Intell. Robots Syst.*, 1995, vol. 1, pp. 399–406.

[38] M. Zinn, O. Khatib, and B. Roth, "A new actuation approach for human friendly robot design," in *Proc. IEEE Int. Conf. Robot. Autom.*, 2004, vol. 1, pp. 249–254.

[39] J. Park, B. Kim, J. Song, and H. Kim, "Safe link mechanism based on passive compliance for safe human-robot collision," in *Proc. IEEE Int. Conf. Robot. Autom.*, 2007, pp. 1152–1157.

[40] A. Albu-Schaffer *et al.*, "Soft robotics," *IEEE Robot. Autom. Mag.*, vol. 15, no. 3, pp. 20–30, Sep. 2008.

[41] F. Lotti, P. Tiezzi, G. Vassura, L. Biagiotti, G. Palli, and C. Melchiorri, "Development of UB Hand 3: Early results," in *Proc. IEEE Int. Conf. Robot. Autom.*, 2005, pp. 4488–4493.

[42] T. D. Niehues, P. Rao, and A. D. Deshpande, "Compliance in parallel to actuators for improving stability of robotic hands during grasping and manipulation," *Int. J. Robot. Res.*, vol. 34, no. 3, pp. 256–269, 2015.

[43] R. Ozawa, H. Kobayashi, and K. Hashirii, "Analysis, classification, and design of tendon-driven mechanisms," *IEEE Trans. Robot.*, vol. 30, no. 2, pp. 396–410, Apr. 2014.

[44] N. Dechev, W. Cleghorn, and S. Naumann, "Multiple finger, passive adaptive grasp prosthetic hand," *Mechanism Mach. Theory*, vol. 36, no. 10, pp. 1157–1173, 2001.
[45] B. Massa, S. Roccella, M. C. Carrozza, and P. Dario, "Design and development of an underactuated prosthetic hand," in *Proc. IEEE Int. Conf. Robot. Autom.*, Washington, DC, USA, 2002, vol. 4, pp. 3374–3379.
[46] C. H. Xiong, W. R. Chen, B. Y. Sun, M. J. Liu, S. G. Yue, and W. B. Chen, "Design and implementation of an anthropomorphic hand for replicating human grasping functions," *IEEE Trans. Robot.*, vol. 32, no. 3, pp. 652–671, Jun. 2016.
[47] J. W. Grizzle, J. Hurst, B. Morris, H. Park, and K. Sreenath, "MABEL, a new robotic bipedal walker and runner," in *Proc. Amer. Control Conf.*, 2009, pp. 2030–2036.
[48] V. Duindam, A. Macchelli, S. Stramigioli, and H. Bruyninckx, *Modeling and Control of Complex Physical Systems: The Port-Hamiltonian Approach*. Berlin, Germany: Springer, 2009.
[49] K. Liu, C.-H. Xiong, L. He, W.-B. Chen, and X.-L. Huang, "Postural synergy based design of exoskeleton robot replicating human arm reaching movements," *Robot. Auton. Syst.*, vol. 99, pp. 84–96, 2018.
[50] B. Mosadegh *et al.*, "Pneumatic networks for soft robotics that actuate rapidly," *Adv. Funct. Mater.*, vol. 24, no. 15, pp. 2163–2170, 2014.
[51] P. Polygerinos *et al.*, "Modeling of soft fiber-reinforced bending actuators," *IEEE Trans. Robot.*, vol. 31, no. 3, pp. 778–789, Jun. 2015.
[52] M. Ciocarlie *et al.*, "The Velo gripper: A versatile single-actuator design for enveloping, parallel and fingertip grasps," *Int. J. Robot. Res.*, vol. 33, no. 5, pp. 753–767, 2014.

Wenrui Chen received the B.S. and Ph.D. degrees in mechanical engineering from the Huazhong University of Science and Technology, Wuhan, China, in 2010 and 2017, respectively.

In 2016, he was a Visiting Scholar with the University of Lincoln, Lincoln, U.K. Since 2017, he has been an Assistant Professor of Robotics with the College of Electrical and Information Engineering, Hunan University, Changsha, China. His research interests include bioinspired robotics, underactuated compliant mechanisms, and robotic dexterous manipulation.

Caihua Xiong received the Ph.D. degree in mechanical engineering from the Huazhong University of Science and Technology (HUST), Wuhan, China, in 1998.

From 1999 to 2003, he was with the City University of Hong Kong and the Chinese University of Hong Kong, Hong Kong, as a Postdoctoral Fellow, and with the Worcester Polytechnic Institute, Worcester, MA, USA, as a Research Scientist. He is currently a Chang Jiang Professor with HUST, the owner of National Science Fund for Distinguished Young Scholars of China, and the Director of the Institute of Rehabilitation and Medical Robotics, HUST. His research interests include biomechatronic prostheses, rehabilitation robotics, and robot motion planning and control.

Yaonan Wang received the Ph.D. degree in electrical engineering from Hunan University, Changsha, China, in 1994.

From 1994 to 1995, he was a Postdoctoral Research Fellow with the Normal University of Defence Technology, Changsha, China. From 1998 to 2000, he was a Senior Humboldt Fellow in Germany. From 2001 to 2004, he was a Visiting Professor with the University of Bremen, Bremen, Germany. Since 1995, he has been a Professor of Control Engineering with the College of Electrical and Information Engineering, Hunan University. He is an Academician of the Chinese Academy of Engineering. His research interests include robotics, intelligent control, and machine vision.